J. Am. Chem. Soc. **1997,** *119,* 4338−4344

Stereodependent Fusion and Fission of Vesicles: Calcium Binding of Synthetic Gemini Phospholipids Containing Two Phosphate Groups

N. A. J. M. Sommerdijk, T. H. L. Hoeks, M. Synak, M. C. Feiters, R. J. M. Nolte,* and B. Zwanenburg*

Contribution from the Department of Organic Chemistry, NSR-Center for Molecular Structure, Design and Synthesis, University of Nijmegen, Toernooiveld, 6525 ED Nijmegen, The Netherlands

Received July 5, 1996. Revised Manuscript Received March 11, 1997[⊗]

Abstract: Three different stereoisomers of a phosphatidic acid analog bearing two phosphate groups have been synthesized from tartaric acid and erythritol. The obtained diastereomeric gemini surfactants differ in their aggregation behavior due to the different spatial orientations of their functional groups. The most remarkable difference in aggregation behavior is encountered when calcium ions are added to vesicle suspensions of the respective isomers. The vesicles formed from the (*S,S*) and *(R,R)* isomer undergo fusion, whereas those of the (*R,S*) isomer show vesicle fission. This remarkable behavior can be explained by a change in the molecular packing of the lipid molecules upon the complexation with calcium ions. An analysis of physical data obtained prior to and after the addition of the calcium ions reveals that the head groups of the diastereomeric surfactants respond differently to these ions: those of the *(S,S)* isomer increase in size, whereas those of the (*R,S*) isomer decrease in size. This phenomenon accounts for occurrence of fusion and fission of the vesicles, respectively.

Introduction

Cell fusion and fission processes are thought to proceed through the binding of calcium ions to acidic phospholipid molecules present in the cell membrane.[1] Most of these lipids contain only one phosphate group, and calcium binding most probably induces dimer formation.[2] These dimers form solid domains in the fluid membrane, allowing other lipids to express their tendency to form nonlamellar structures, leading to the generation of a hexagonal phase as an intermediate state in the fusion or fission process. The effect of calcium and other divalent ions on the aggregation behavior of pure as well as mixed native phospholipids has been studied extensively.[1−3] More recently,[4] vesicle fusion has been demonstrated for synthetic phospholipids after addition of calcium ions. Cytomimetic organic chemistry has shown furthermore that aggregation, fusion, fission, and budding processes can be accomplished in vesicles of cationic surfactants,[5] and that the autocatalytic hydrolysis of oleic anhydride in oleic acid vesicles even can yield a self-reproducing system.[6]

A study of the influence of calcium ions on vesicle systems of surfactants containing acidic phosphate functions seems the most direct approach to the understanding of the mechanisms of the fusion and fission processes in living cells. In most cases, however, the precipitation of their calcium complexes limits the utility of pure acidic phospholipids in mimicking these processes. In this context, the influence of calcium ions on the aggregation behavior of the phosphatidic acid analogs **1** is of interest. These compounds, which also exhibit carries reducing activity,[7] are structurally related to phosphatidic acid but have two, instead of one, phosphate groups. Surfactants of this type are called gemini surfactants and are currently receiving great interest.[8] The formation of 1:1 complexes, rather than dimers, could be expected upon addition of calcium ions to the aggregates of these compounds.

In this paper the synthesis of the stereoisomeric compounds **1a−c** and their aggregation behavior in water is reported. It will be shown that the addition of calcium ions strongly affects the self-assembling properties of these surfactants and that vesicles prepared from **1b** or **1c** can be used to mimic the fusion and fission processes of cells. These compounds do not immediately precipitate after calcium binding, due to the presence of the two phosphate groups, and the processes of both fusion and fission can be monitored by electron microscopy. A

[⊗] Abstract published in *Advance ACS Abstracts,* May 1, 1997.

(1) (a) Gingel, D.; Ginsberg, L. In *Cell Surface Rev.* Poste, G., Nicolson, G. L., Eds.; North Holland, Amsterdam, 1978; Vol. 5, pp 791−833. (b) Cullis, P. R; de Kruijff, B. *Biochim. Biophys. Acta* **1979**, *559*, 399. (c) *Molecular mechanisms of membrane fusion*; Ohki, S., Doyle, D., Flanagan, T. D., Hui, S. W., Mayhew, E., Eds.; Plenum: New York, 1988.

(2) Ohnishi, T.; Ito, T. *Biochemistry* **1974**, *13*, 881.

(3) (a) Verkleij, A. J.; De Kruyff, B.; Ververgaert, P. H. J. Ph.; Tocanne, J. F.; van Deenen, L. L. M. *Biochim. Biophys. Acta* **1974**, *339*, 432. (b) Papahadjopoulos, D.; Jacobson, K.; Vail, W. J.; Poste, G. *Biochim. Biophys. Acta* **1975**, *394*, 483. (c) Papahadjopoulos, D.; Vail, W. J.; Pangborn, W. A.; Poste, G. *Biochim. Biophys. Acta* **1976**, *448*, 265. (d) Dluhy, R. A.; Cameron, D. G.; Mantsch, H. H.; Mendelsohn, R. *Biochemistry* **1983**, *22*, 6318. (e) Verkleij, A. J. *Biochim. Biophys. Acta* **1984,** *779*, 43. (f) Nakashima, N.; Ando, R.; Fukushima, H.; Kunitake, T. *Chem. Lett.* **1985**, 1503. (g) Siegel, D. P. *Biophys. J.* **1986**, *49*, 1171. (h) Casal, H. L.; Marin, A.; Mantsch, H. H.; Paltauf, F.; Hauser, H. *Biochemistry* **1987**, *26*, 4408. (i) Casal, H. L.; Mantsch, H. H.; Hauser, H. *Biochemistry* **1987**, *26*, 7395. (j) Casal, H. L.; Mantsch, H. H.; Hauser, H. *Biochim. Biophys. Acta* **1989**, *982*, 228.

(4) (a) Rupert, L. A. M.; van Breemen, J. F. L.; van Bruggen, E. F. J.; Engberts, J. B. F. N. Hoekstra, D. *J. Membrane Biol.* **1987**, *95*, 225. (b) Wagenaar, A.; Streefland, L.; Hoekstra, D.; Engberts, J. B. F. N. *J. Phys. Org. Chem.* **1992**, *5*, 451. (c) Streefland, L. Wagenaar, A. Hoekstra, D. Engberts, J. B. F. N. *Langmuir* **1993**, *9*, 219.

(5) (a) Rupert, L. A. M.; Engberts, J. B. F. N.; Hoekstra, D. *J. Am. Chem. Soc.* **1986**, *107*, 2628. (b) Rupert, L. A. M.; Engberts, J. B. F. N.; Hoekstra, D. *J. Am. Chem. Soc.* **1986**, *108*, 3920. (c) Menger, F. M.; Balachander, N. *J. Am. Chem. Soc.* **1992**, *114*, 5862. (d) Menger, F. M.; Gabrielson, K. *J. Am. Chem. Soc.* **1994**, *11*, 1567. (e) Menger, F. M.; Gabrielson, K. D *Angew. Chem.* **1995**, *107*, 2260.

(6) Wick, R.; Wade, P.; Luisi, P. L. *J. Am. Chem. Soc.* **1995**, *117*, 1435.

(7) Borggreven, J. M. P. M.; Hoeks, T. H. L.; Driessens, F. C. M.; Zwanenburg, B. *Caries Res.* **1992**, *26*, 84.

(8) (a)Menger, F. M.; Littau, C. A. *J. Am. Chem. Soc.* **1993**, *115*, 10083. (b) Karaborni, S.; Esselink, K.; Hilbers, P. A. J.; Smit, B.; Karthäuser, J.; van Os, N. M.; Zana, R. *Science* **1994**, *266*, 254.

S0002-7863(96)02303-7 CCC: $14.00

Scheme 1

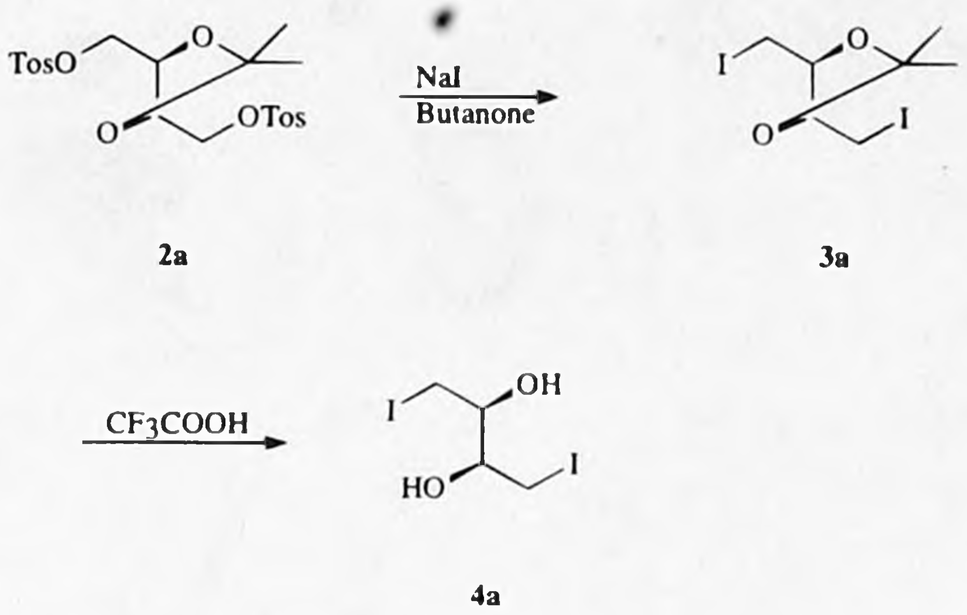

Scheme 2

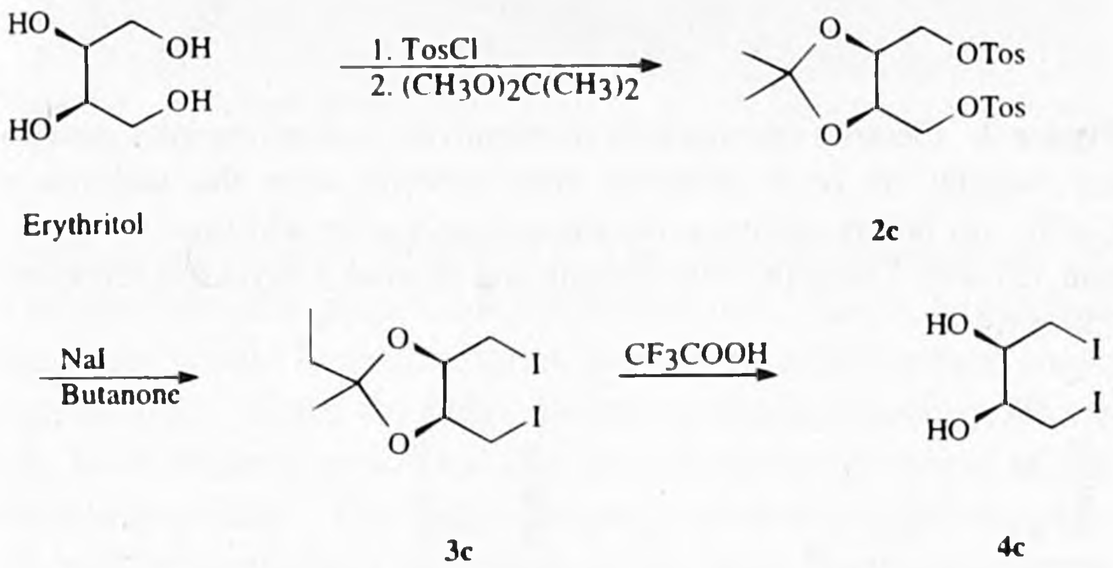

discussion of the mechanisms of these processes based on the shape and physical properties of the aggregates before and after addition of the calcium ions is presented.

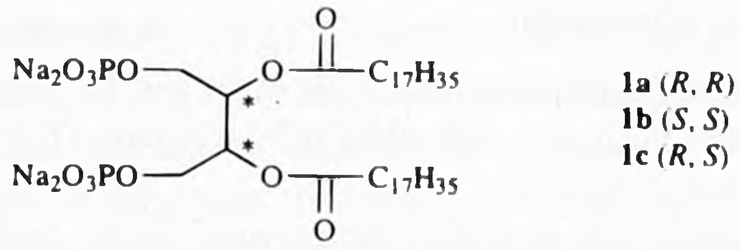

Results and Discussion

Synthesis. Compounds **1** were synthesized by acylation and subsequent phosphorylation of the respective secondary diiodo alcohols in order to avoid both acyl migration[9] and cyclic phosphate formation.[10] Diiodobutanediols **4** were prepared from the corresponding 2,3-isopropylidene-1,4-ditosylates **2** (Schemes 1 and 2).

The optically active ditosylates **2a**,**b** were obtained from D-(−)- and L(+)-tartaric acid, respectively, using literature procedures (Scheme 1).[11−13] The conversion of **2a**,**b** into the corresponding diiodides **3a**,**b** using sodium iodide in butanone proceeded smoothly, and mild hydrolysis with trifluoroacetic acid in aqueous methanol afforded the diols **4a**,**b** in 97% overall yield.

Meso compound **2c** was obtained (52%) from erythritol by selective tosylation of the primary hydroxyl groups and subsequent protection of the secondary hydroxyl groups using 2,2-

Scheme 3

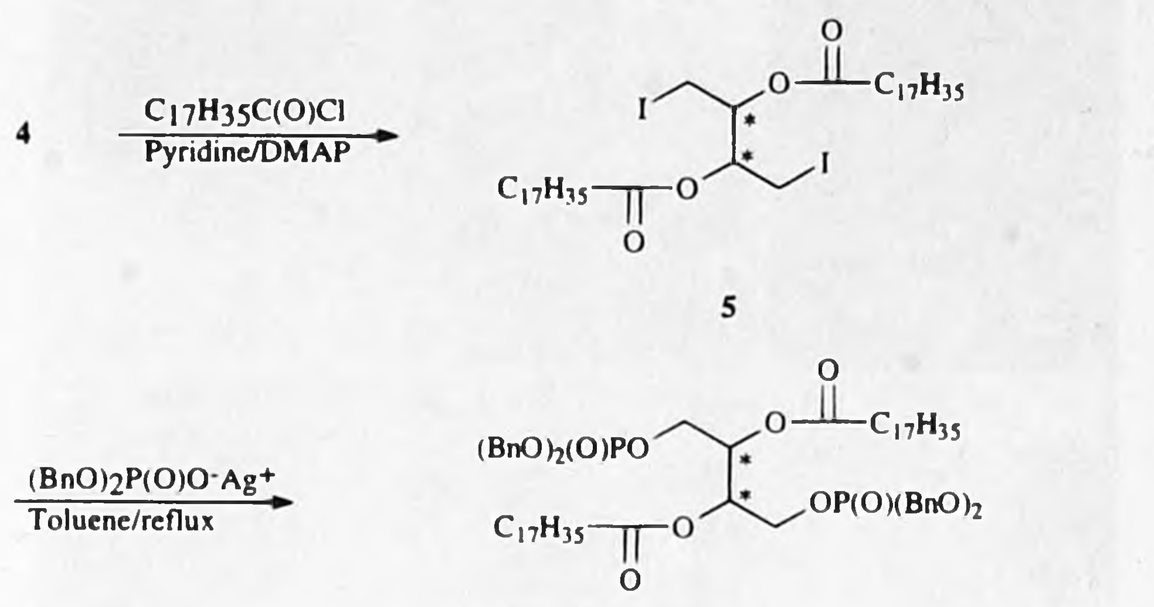

dimethoxypropane (Scheme 2).[14] During the reaction of **2c** with sodium iodide in butanone concurrent trans-acetalization occurred, probably due to the presence of traces of iodine.[15] The two diastereomers of the corresponding isobutylidene derivative **3c** were not purified but were directly subjected to hydrolysis to give **4c** in 94% overall yield.

Acylation of diiodides **4** was performed in 95−97% yield with fatty acid chlorides in pyridine using *N*,*N*-dimethylaminopyridine (DMAP) as the catalyst (Scheme 3). Reaction of diiodo esters **5** with silver dibenzyl phosphate in refluxing toluene afforded the corresponding phosphotriesters in good yields.[16] Catalytic hydrogenolysis and subsequent ion exchange gave the respective tetrasodium salts **1** which, after lyophilization, were isolated as white amorphous powders.[17]

Aggregation Behavior and Calcium Binding. All three stereoisomers of **1** formed planar bilayers after dispersion in water of pH = 7.0 by vortexing at 70 °C, as was demonstrated by electron microscopy (not shown).[18] Since **1a** and **1b** are enantiomers and have therefore identical physical properties (apart from their optical properties), only **1b** and **1c** were used in aggregation experiments described below.

Sonication of an aqueous 0.1% (w/w) dispersion of the (*S*,*S*) isomer **1b** led to the formation of very small unilamellar vesicles with diameters of 15−25 nm (Figure 1a). When calcium ions were added to the sonicated dispersion of **1b**, fusion of the vesicles occurred, resulting in larger vesicles with diameters of 50−100 nm (Figure 1).[19] This process was monitored by preparing samples for electron microscopy at different stages after the addition of the calcium ions. It can be deduced from

(9) (a) Fischer, E. *Ber.* **1920**, *53*, 1621. (b) Doerschuk, A. P. *J. Am. Chem. Soc.* **1952**, *74*, 4202. (c) van Lohuizen, O. E.; Verkade, P. E. *Recl. Trav. Chim. Pays-Bas* **1960**, *79*, 133. (d) Serdavich, B. *J. Am. Oil Chem. Soc.* **1967**, *44*, 1.

(10) (a) Brown, D. M.; Magrath, D. I.; Todd, A. R. *J. Chem. Soc.* **1955**, 4396. (b) de Rooy, J. F. M.; Wille-Hazeleger, G.; Burgers, P. M. J.; Van Boom, J. H. *Nucleic Acids Res.* **1979**, *6*, 2237.

(11) Carmack, M.; Kelly, C. J. *J. Org. Chem.* **1968**, *33*, 2171.

(12) Seebach, D.; Hungerbühler, E. *Modern Synthetic Methods*; Sheffold, R., Ed.; Otto Salle Verlag, Frankfort/Munich 1980; Vol. 2, p 155.

(13) Rubin, L. J.; Lardy, H. A.; Fischer, H. O. L. *J. Am. Chem. Soc.* **1952**, *74*, 425.

(14) Direct iodination of 1,4-ditosyl erythritol led to the formation of 1-iodo-3,4-buten-2-ol (see, also: House, H. O.; Ro, R. S. *J. Am. Chem. Soc.* **1958**, *80*, 182. Cristol, S. J.; Rademacher, L. E. *J. Am. Chem. Soc.* **1959**, *81*, 1600.)

(15) (a) Szarek, W. A.; Zamojski, A.; Tiwari, K. M.; Ison, E. R. *Tetrahedron Lett.* **1986**, 3827. (b) Verhart, C. G. J.; Caris, B. M. G.; Zwanenburg, B.; Chittenden, G. J. F. *Rec. Trav. Chim. Pays-Bas* **1992**, *110*, 348.

(16) Zervas, L. *Naturwiss.* **1939**, *27*, 317.

(17) The enantiomeric purity of **1a**,**b** was checked by ^{1}H-NMR analysis of the corresponding methyl esters using Eu(hfc)$_3$ as a chiral shift reagent. Methylation was accomplished by reaction of the free acid of **1a,b** with diazomethane. Enantiomeric splitting of the methyl signals revealed an optical purity of at least 95%.

(18) Sommerdijk, N. A. J. M.; Feiters, M. C.; Nolte, R. J. M.; Zwanenburg, B. *Recl. Trav. Chim. Pays-Bas* **1994**, *113*, 194.

(19) Control experiments were performed using **1a.** These experiments revealed that this compound also exhibits vesicle fusion upon addition of calcium ions.

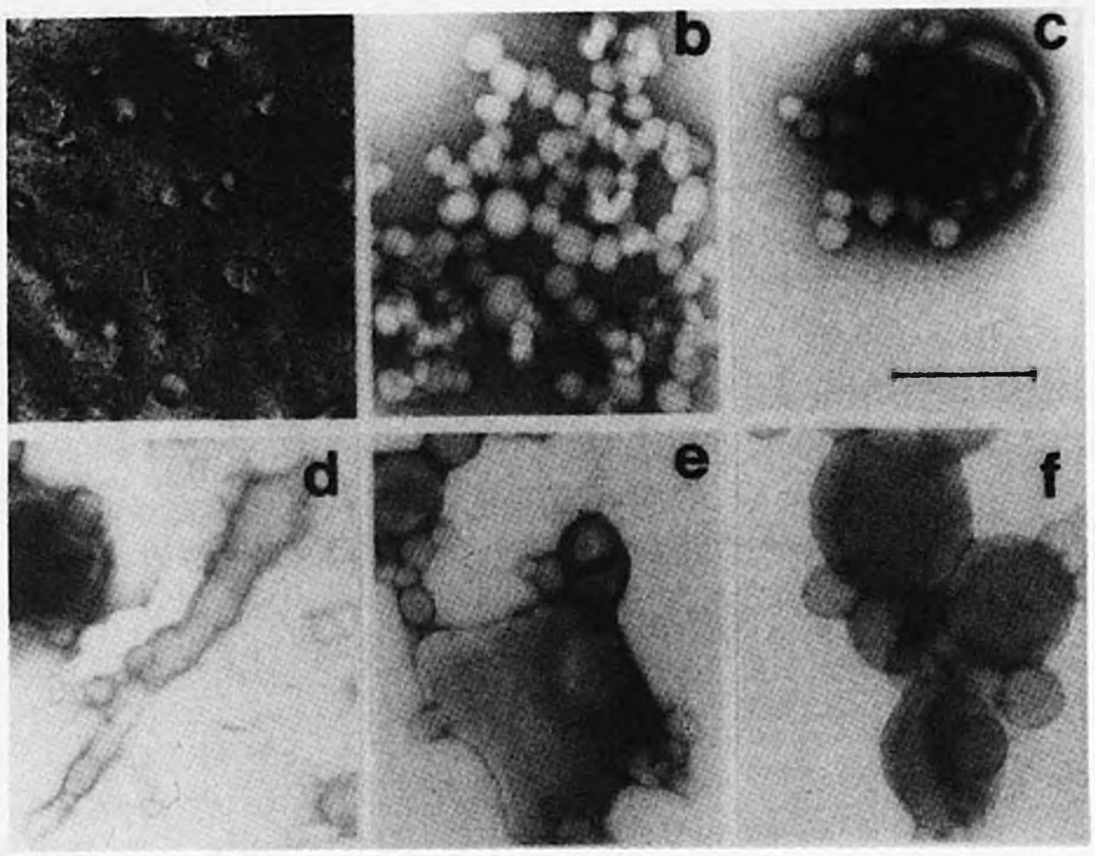

Figure 1. Electron micrographs of samples containing vesicles of **1b** at different time intervals after the addition of $CaCl_2$: (a) freeze fracture and (b−f) negative staining. (a) Before addition, (b) immediately after addition, (c-d) after 20 min, and (e-f) after 2 h. Bar represents 100 nm.

Table 1. DSC Data Obtained from Aqueous 1% (w/w) Dispersions of **1**, Before and After Addition of a Calcium Chloride Solution (See Experimental Section)

compd	T^a (°C)	ΔH (J/g)	ΔS (J/g·K)
1b → **1b**/Ca^{2+}	8 → 42	88 → 10	0.31 → 0.03
1c → **1c**/Ca^{2+}	38 → 41	66 → 3	0.21 → 0.01

[a] Onset temperature.

Figure 1b that clustering of the vesicles occurs immediately after addition of the ions. The subsequent fusion process was trapped in different stages, showing both the incorporation of various small vesicles into a larger one (Figure 1c) and the simultaneous fusion of several small vesicles (Figure 1d,e). In contrast to other systems,[5c] the clustering of the vesicles is probably not the rate limiting factor, since after two hours the fusion process was still not complete (Figure 1f).

DSC experiments showed that the addition of calcium ions caused an increase in the gel to liquid−crystalline phase transition temperature (Table 1). The transition entropy, calculated from these data, decreased remarkably from 0.3 J/(g·K) to 0.03 J/(g·K), indicating drastic changes in the organization of the bilayer.

Cast films of 0.1% (w/w) dispersions of the (*S,S*) isomer **1b** were found to consist of intercalated bilayers with a thickness of 38 ± 2 Å, as determined from the higher order reflections in wide angle powder diffraction patterns.[18] A different diffraction pattern was obtained after addition of calcium ions, but analysis of the data indicated the same bilayer thickness (d = 38 ± 2 Å).

Sonication of aqueous dispersions of *meso* compound **1c** led to the formation of unilamellar vesicles with a diameter of 50−100 nm (Figure 2). After addition of calcium ions, fission of the vesicles occurred, leading to the formation of much smaller vesicles with diameters of 10−25 nm. This process was found to be relatively fast, compared with the fusion process described above, being complete after 20 min. During this process, irregular curved structures were formed, from which small vesicles were blebbing off. These vesicles transformed into tubular structures with a length of several micrometers and a diameter of approximately 10−20 nm (Figure 2f) on being set aside for several days.

Dispersions prepared from **1c** displayed a gel to liquid−crystalline phase transition at 38 °C in DSC experiments (Table 1). These vesicles contained bilayers with a thickness of 38 ± 2 Å according to powder diffraction data, indicating an intercalation of the hydrocarbon chains, similar to the structures formed from **1b**. The addition of $CaCl_2$ led only to a minor shift of the phase transition temperature, but a distinct decrease in transition entropy was observed (Table 1). A bilayer thickness of 66 ± 1 Å was calculated from powder diffraction data, which suggests a reorganization of the lamellae resulting in a normal nonintercalated bilayer structure.

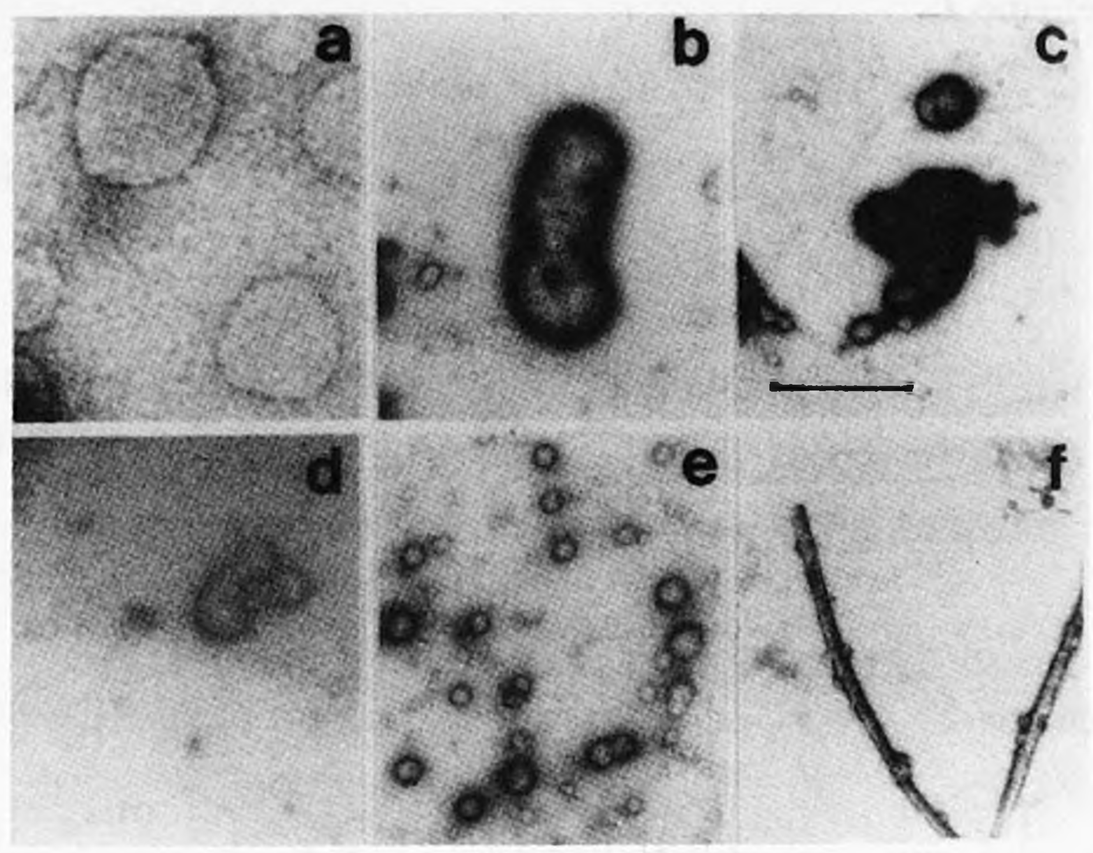

Figure 2. Electron micrographs of negatively stained samples containing vesicles of **1c** at different time intervals after the addition of $CaCl_2$: (a) before addition, (b) immediately after addition, (c) after 1 min, (d) after 3 min, (e) after 30 min, and (f) after 3 days. Bar represents 250 nm.

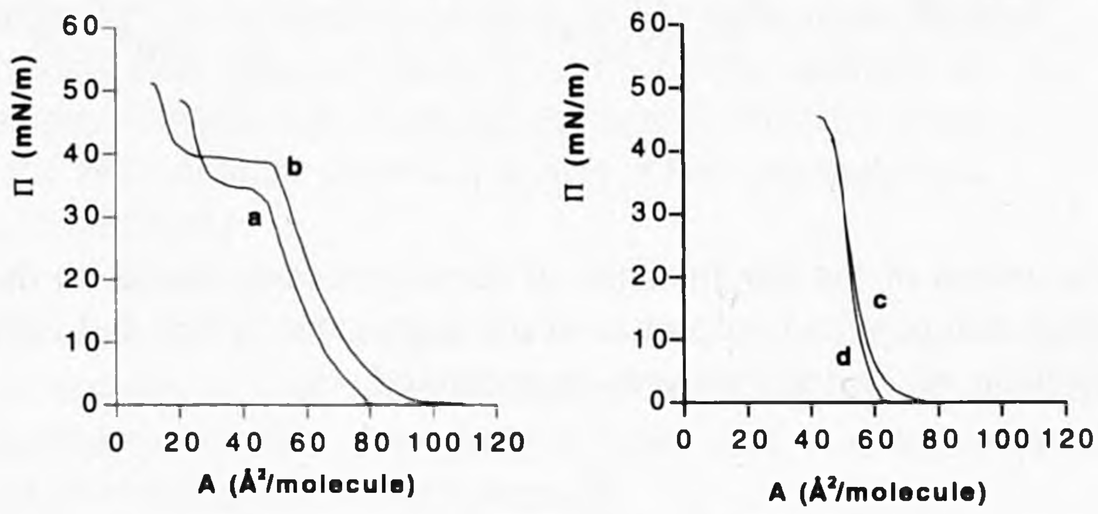

Figure 3. Monolayer isotherms of **1b** (left) and **1c** (right) on (a, c) pure water and on (b, d) a 1.0 mM $CaCl_2$ subphase (T = 20 °C).

Monolayer Experiments. Monolayer experiments were then performed with **1** in order to gain insight into the effect of calcium binding on the size of the polar head groups of these surfactants. *Meso* compound **1c**, after being spread on an aqueous subphase, occupied a smaller area than (*S,S*) isomer **1b** (Figure 3a and 3c). The Π-A diagram of **1b** showed a plateau starting at 45 Å^2 per molecule and after further compression again an increase in surface pressure. This plateau may be interpreted as the result of a collapse of the monolayer since the minimum area to which two alkyl chains can be compressed amounts to approximately 38 Å^2. Brewster angle microscopy[20] did not give evidence for a collapse in this region; however, a continued densification of the surface was observed. This might be explained by a gradual formation of a bilayer, which is supported by the increase in surface pressure upon further compression and the observation of a collapse at an area of approximately 20 Å^2 per molecule.

Information about the most favorable spatial orientation of the respective substituents in the various conformations of compounds **1b** and **1c** can be obtained from an analysis of their

(20) (a) Hénon, S.; Meunier, J. *Rev. Sci. Intrum.* **1991**, *62*, 936. (b) Hönig, D.; Möbius, D. *J. Phys. Chem.* **1991**, *95*, 4590.

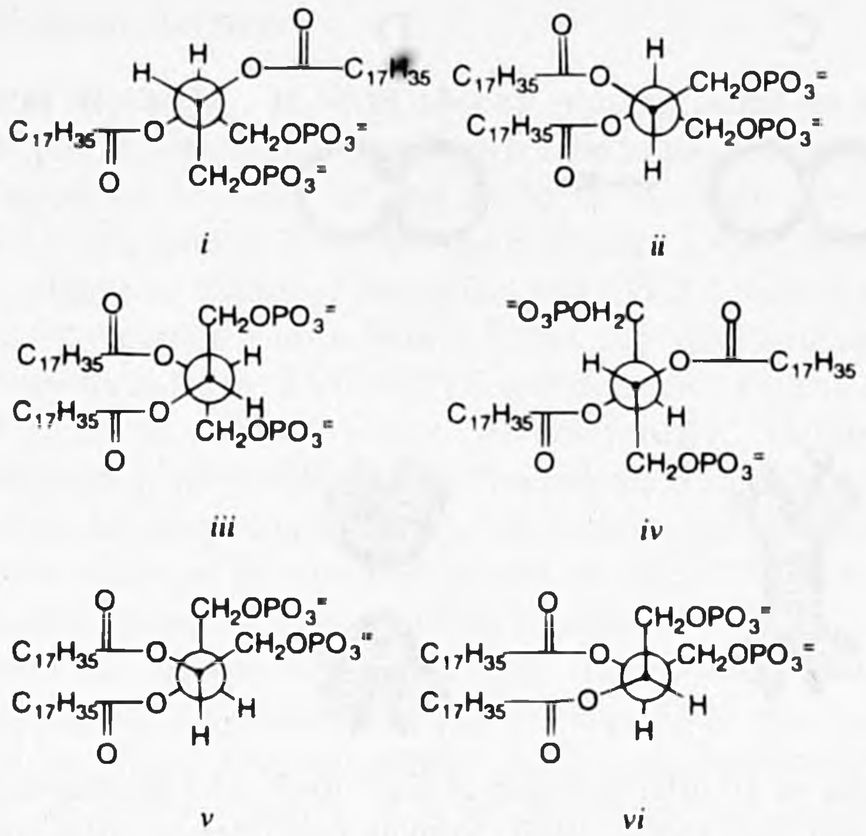

i *ii* *iii* *iv* *v* *vi*

Figure 4. Newman projections of **1b** (*i*, *ii*, and *iii*) and **1c** (*iv*, *v*, and *vi*).

Newman projections (Figure 4). The conformations *i* and *iv*, in which the ester groups are positioned *anti*, can be neglected, since they would be unfavorable in terms of hydrocarbon chain organization. Thus, for (*S,S*)-**1b** the remaining conformations may have either a *gauche* (*ii*) or an *anti* (*iii*) orientation of the phosphate groups. The latter, although more sterically demanding, will be more favorable, since it will have the lowest degree of electrostatic repulsion. For the (*R,S*) isomer **1c** both *v* and *vi* will lead to a *gauche* orientation of the phosphate groups. This explains the relatively small molecular area occupied by this molecule as compared to **1b**. Both conformations *v* and *vi* of **1c** lead to an overall "L"-shape for the molecule, whereas the *anti* conformation *iii* of **1b** leads to a "T"-shape.

The isotherms of **1b** and **1c** revealed a remarkable difference in the response toward the addition of calcium ions (Figure 3b and d). When a subphase containing 1.0 mM calcium chloride was used instead of water, the molecular area of (*R,S*) isomer **1c** decreased, whereas the (*S,S*) isomer **1b** showed a surprising increase in area per molecule.

These findings can be explained by the binding of a calcium ion to two phosphate groups of the same molecule in the case of **1c** (Figure 5b), leading to a more compact conformation of the molecule, and the intermolecular binding to two phosphate groups of different molecules in the case of **1b** (Figure 5a). The latter will lead to a polymeric type of structure giving rise to a more stretched-out conformation with a larger molecular area.

These differences in behavior upon binding of calcium ions may be rationalized by considering again the differences in geometric orientation of the phosphate groups in these two diastereomeric compounds. The *meso* compound **1c** will be a better chelating agent than **1b**, due to its preference for *gauche* conformations as discussed above. Compound **1b** prefers a conformation *iii* in which the two phosphate groups are *antiperiplanar*.

Discussion of the Mechanisms of Fusion and Fission. The physical data obtained from the experiments described above can also be used to rationalize the difference in response during addition of calcium ions to vesicle dispersions of the respective diastereomers. The assumed formation of a polymeric type of complex (Figure 5a) will stabilize the membrane structure of **1b**, allowing larger aggregates to be formed. A reduction in surface charge will decrease electrostatic repulsion between the vesicles. Aggregation (Figure 6B-I) may then lead to the formation of intervesicular calcium complexes (Figure 6B-II). Subsequent withdrawal of the outer bilayer halves (Figure 6B-III) and merging of the two inner halves will produce a new intercalated bilayer (Figure 6C). Cleavage of this bilayer eventually yields the new vesicle (Figure 6D).

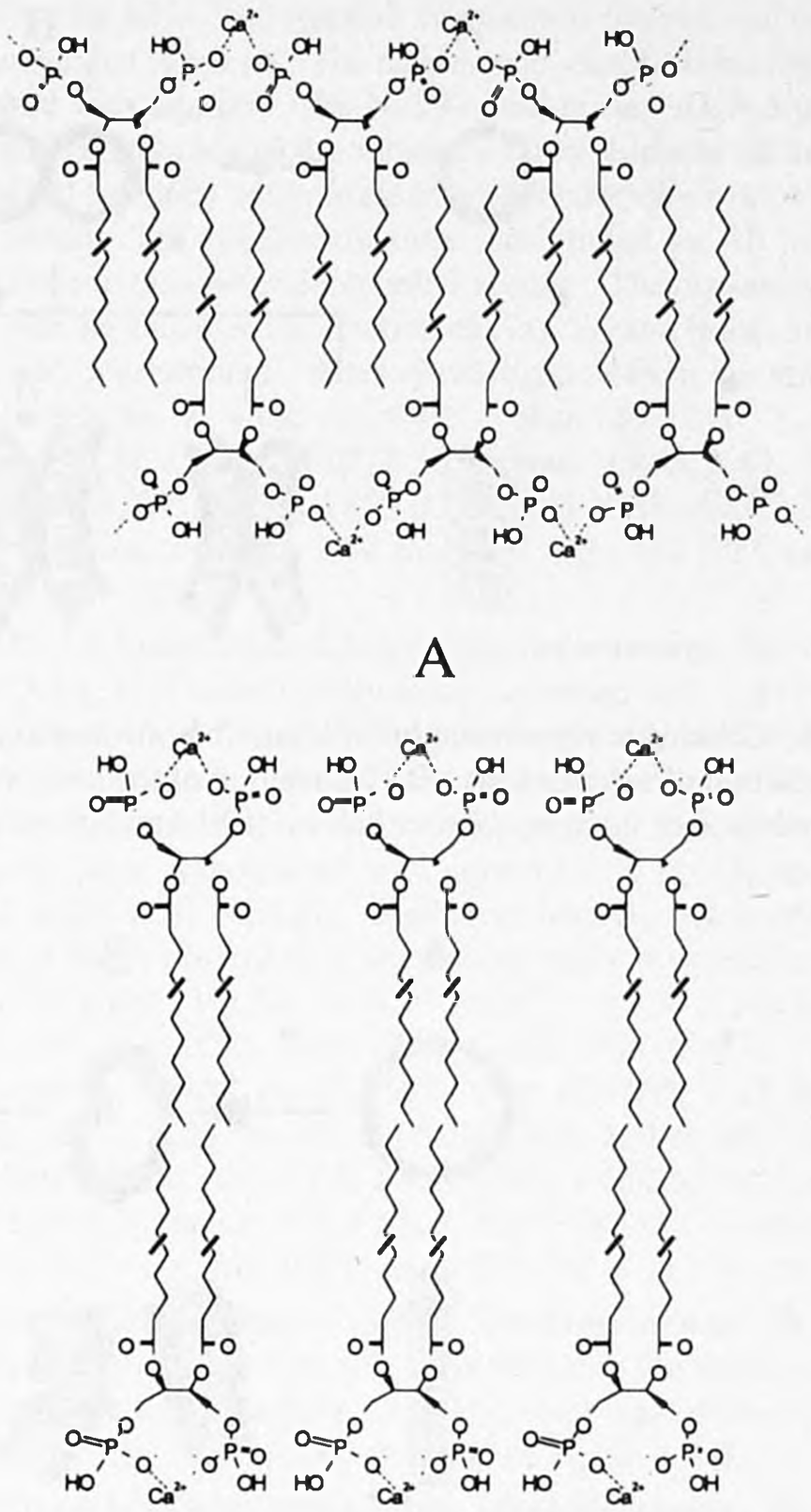

A

B

Figure 5. Proposed bilayer structures in the case of (A) **1b** and (B) **1c** after addition of calcium ions. Intermolecular complexation of calcium ions (A) gives rise to a more stretched out conformation of the head groups, whereas intramolecular complexation (B) of calcium ions gives rise to a more compact conformation.

Chelate formation decreases the molecular area of **1c**, leaving insufficient space to accommodate four hydrocarbon chains. This will destabilize the intercalated structure of the original bilayer (Figure 7). Transformation to a normal lamellar structure will, because of the conical shape of the molecules, lead to the formation of strongly curved bilayer fragments which are thermodynamically unstable (Figure 7B). Smaller vesicles with a lower degree of hydrocarbon chain packing are formed by the blebbing off of these fragments (Figure 7C−E). These vesicles will adopt a thermodynamically more stable organization upon standing, resulting in the formation of tubular structures.[21]

In the case of compound **1b**, intermolecular complexation will cause an increase in molecular area as the molecules have to adopt a more stretched-out conformation. Since no change in the thickness of the bilayer was observed, it must be concluded that this process leads to a lower degree of hydrocarbon chain packing.[22] This disorder in the bilayer interior will render the aggregates more fluid and will prevent the precipitation of the complexes. With compound **1c** the formation of a calcium complex will lead to a smaller spatial demand

(21) These events have been observed in reversed order for the fusion of ammonium surfactants. See ref 5d.

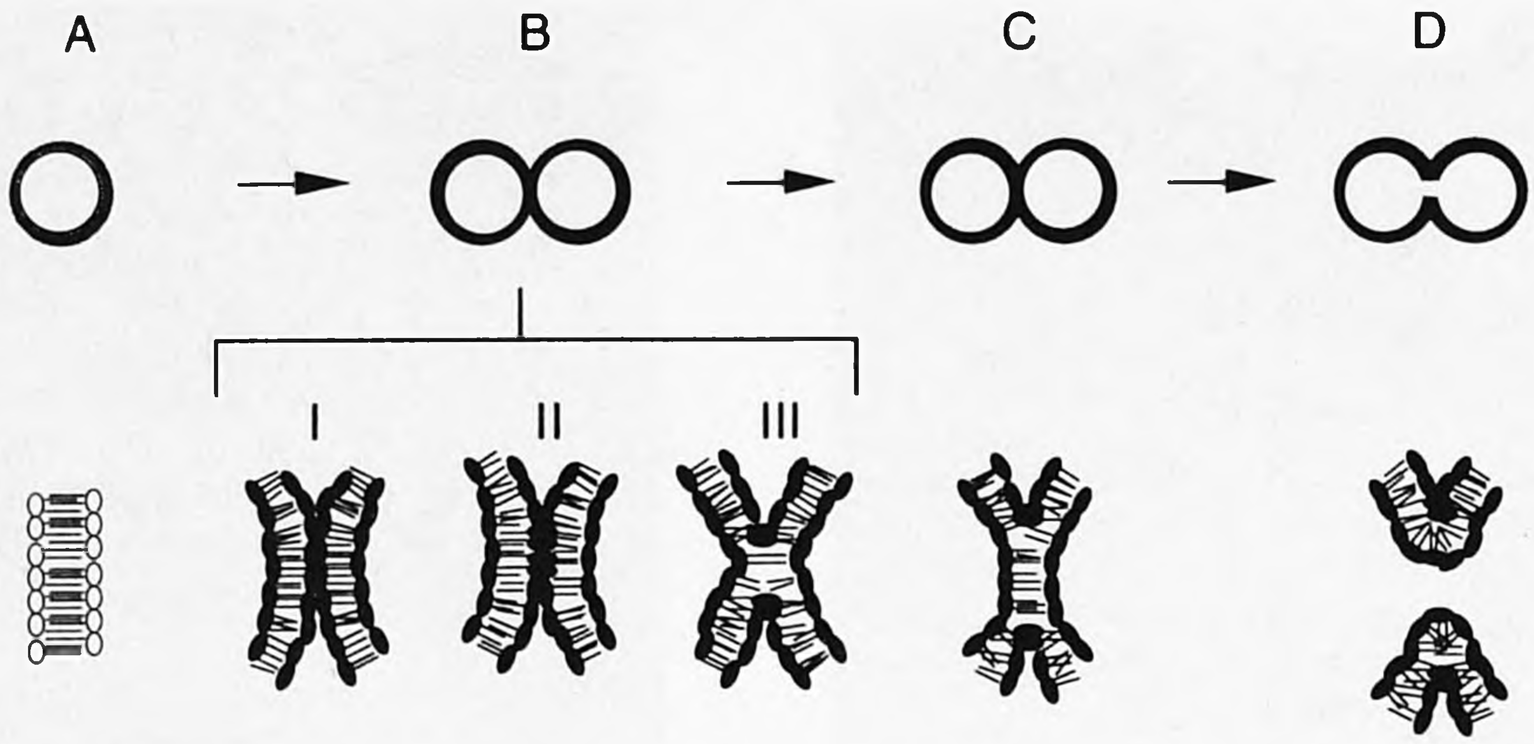

Figure 6. Schematic representation of a possible mechanism for the fusion of vesicles of **1b** after addition of Ca^{2+} ions: (A) intercalated bilayer before addition of calcium ions, (B-I) clustering of the vesicles after reduction of the repulsive forces, (B-II) formation of intervesicular complexes, (B-III) redrawal of the outer bilayer halves, (C) formation of a new intercalated bilayer, and (D) the merging of the vesicles by cleavage of the new bilayer.

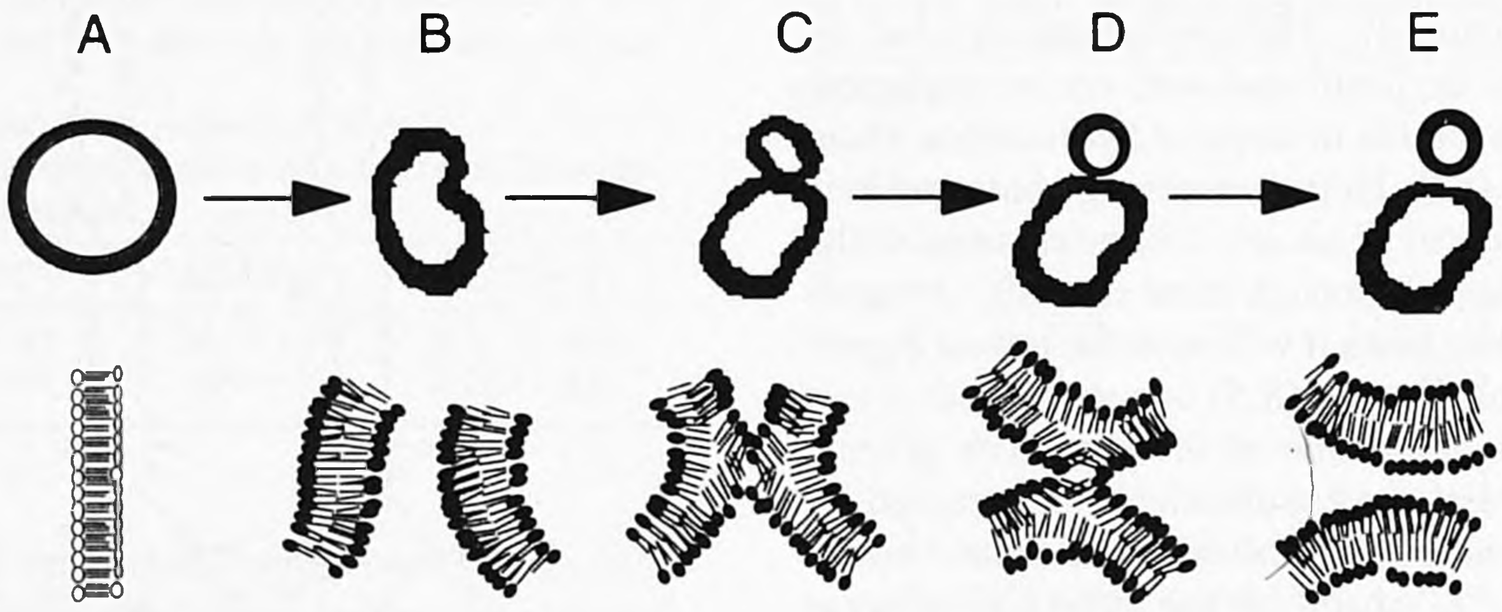

Figure 7. Schematic representation of a possible mechanism for the fission of vesicles of **1c** after the addition of calcium ions: (A) intercalated bilayer before addition of calcium ions, (B) decrease of the head group size causes a transformation to a highly curved, nonintercalated bilayer, (C) reduced electrostatic repulsion alows contact of the head groups from different parts of the inner bilayer half, (D) head groups of the molecules will redirect to the aqueous phase which, by merging of the bilayers, (E) leads to the blebbing off of a small vesicle.

of the lipophilic part since the alkyl chains are no longer intercalated and hence to the formation of aggregates with a low hydrocarbon chain organization in the interior of the bilayer.[22] No precipitation of the complex is observed initially, but precipitation occurs after several days when the vesicles have transformed into the more stable tubular structures.

Conclusion

The experiments described above, reveal that these new gemini surfactants may serve as interesting models for biomembranes. The introduction of an extra phosphate group has a dramatic effect on both the aggregation behavior and on the calcium binding properties of the phosphatidic acids. The increase in the size of the head group leads to the formation of intercalated bilayers from the three different stereoisomers of **1**. The difference in orientation of the phosphate groups in the *meso* and the (*S,S*) diastereomers of **1** leads to a remarkably different response toward calcium ions. Apparently (*S,S*) compound **1b** is not able to form a stable 1:1 chelate for steric reasons but preferentially forms a linear polymeric complex. This eventually leads to fusion of the vesicles. Due to conformational preferences compound **1c** forms a 1:1 chelate, which leads to a destabilization of the intercalated bilayer. A transition to a normal lamellar structure restores the bilayer but requires a highly curved surface, which leads to the fission of the vesicles.

Due to the large head group size of the described phospholipid molecules, which arises from the introduction of a second phosphate group, the calcium complexes show a poor hydrocarbon chain packing. As a result of this, the lamellar structures, formed upon dispersion in water, do not immediately precipitate upon addition of calcium chloride as observed in the case of phosphatidic acids. This enabled the monitoring of the processes of both vesicle fusion and vesicle fission. It was possible to present mechanistic models for the shape of the molecular assemblies during these processes based on the physical data of the aggregates prior to and after addition of calcium ions.

The described vesicular systems show that a small alteration in the orientation of functional groups can give rise to a big change in response to external signals. These experiments demonstrate furthermore that the observed changes in lipid morphologies can be brought about without the action of complex mechanisms involving intermolecular or intercellular interactions but simply by altering the conformational properties of the molecules involved. These insights may be useful in understanding cell fusion and fission processes which are believed to be initiated by similar calcium induced alterations in head group size and the consequent changes in the conformational characteristics of the molecules involved.

(22) The reflection in the 4.0−4.5 Å region represents the side of a cell in the hexagonal lattice in which the hydrocarbon chains are packed. For both compounds a broadening in this reflection is observed after addition of calcium ions. This is indicative of a distorted hydrocarbon chain packing, see: (a) Gulik-Krzywicki, T.; Rivas, E.; Luzzati, V. *J. Mol. Biol.* **1967**, *27*, 303. (b) Tardieu, A.; Luzzati, V. *J. Mol. Biol.* **1973**, *75*, 711. (c) Ranck, J. L.; Mathieu, L.; Sadler, D. M.; Tardieu, A.; Gulik-Krzywicki,; T. Luzzati, V. *J. Mol. Biol.* **1974**, *85*, 249. This decrease in organization in the interior of the membrane is also in agreement with the change in transition entropy deduced from the DSC data (Table 1).

Experimental Section

General Methods. ^{1}H-NMR spectra were recorded on a Bruker AM-400 spectrometer using tetramethylsilane as the internal standard. Proton-decoupled 81 MHz ^{31}P and 50 MHz ^{13}C NMR spectra were obtained using a Bruker WM-200 spectrometer. Chemical shifts are reported relative to trimethyl phosphate and $CDCl_3$, respectively. IR spectra were recorded with a Perkin Elmer 298 spectrometer. Mass spectra were recorded on a VG 7070 E spectrometer. Optical rotations were measured on a Perkin Elmer 241 polarimeter. Melting points were determined using a Reichert Thermopan microscope and are uncorrected. In chromatographic procedures silica gel 60H (Merck art. no. 7736) or silica gel 60 silanated (Merck art. no. 7719) were used as the stationary phase. For ion exchange Dowex 50 W × 2 in Na^+-form (Fluka AG, art. no. 44465) was used. Thin layer chromatograms were run on glass supported silica gel 60 plates (0.25 mm-layer, F_{254}, Merck art. no. 5715). The molybdate[23] and Knight and Young[24] sprays were used as location reagents. Solvents were dried and distilled, when appropriate, using the following methods: diethyl ether, benzene, and dichloromethane were distilled from calcium hydride; toluene was distilled from sodium, pyridine was distilled from sodium hydroxide, and THF was distilled from lithium aluminium hydride. All other solvents used were of analytical grade.

1,4-Ditosyl Erythritol. Erythritol (4 g, 33 mmol) was dissolved in pyridine (80 mL) and cooled to −20 °C. A solution of tosyl chloride (12.5 g, 30 mmol) in dry dichloromethane (40 mL) was added dropwise over a period of 8 h. The reaction mixture was stirred for another 16 h while warming to room temperature. After concentration in vacuo dichloromethane was added to the mixture, and the organic layer was washed with aqueous 1 M sulfuric acid, water, and brine. After drying over $MgSO_4$ and evaporation of the solvent, the mixture was subjected to column chromatography (silica gel, ethyl acetate/hexane 1:1, v/v). After crystallization from chloroform, 1,4-ditosyl erythritol was obtained in 55% yield (mp 88 °C). IR (KBr, cm^{-1}): ν 3500 (O-H), 3020 (C-H arom), 2980, 2920, 2850 (C-H alkyl), 1600 (S=O). ^{1}H-NMR ($CDCl_3$, ppm): δ 1.60 (br.s, 2H, OH), 2.45 (s, 6H, $CH_3C_6H_5$) 4.05 (m, 4H, CH_2), 4.65 (m, 2H, C*H*), 7.25 (d, 4H, H3 and H5 arom, J = 5 Hz), 7.80 (d, 4H, H2 and H6 arom, J = 5 Hz).

1,4-Ditosyl-2,3-*O*-isopropylidene Erythritol, 2c. To a suspension of 1,4-ditosyl erythritol (1.0 g, 2.39 mmol) in 2,2-dimethoxypropane (10 mL) was then added *p*-toluenesulfonic acid (45 mg, 2.4 mmol), and the mixture was stirred for 16 h at room temperature. A saturated aqueous solution of $NaHCO_3$ was added, and the mixture was extracted with ethyl acetate. The organic layer was washed with water and brine, dried over $MgSO_4$, and concentrated in vacuo. Crystallization from ethyl acetate gave pure **2c** in 94% yield (Mp 127−129 °C) Anal. ($C_{21}H_{26}S_2O_8$) C, H, S Calcd: 52.60, 5.57, 13.63. Found: 52.60, 5.37, 13.50. IR (KBr, cm^{-1}): ν 3020 (C-H arom), 2980, 2920, 2850 (C-H alkyl), 1600 (S=O). ^{1}H-NMR ($CDCl_3$, ppm): δ 1.30 (s, 3H, CH_3), 1.32 (s, 3H, CH_3), 2.45 (s, 6H, CH_3Tos) 4.05 (m, 4H, CH_2), 4.30 (m, 2H, C*H*), 7.25 (d 4H, H3 and H5 arom, J = 5 Hz,), 7.80 (d, 4H, H2 and H6 arom, J = 5 Hz). MS (EI, *m/z*): 470 (M^+), 285 (M − CH_2OTos).

(2*R*,3*R*)-1,4-Diiodobutane-2,3-diol, 4a. Compound **3a**[12] (2.75 g, 7.2 mmol) was added to a mixture of trifluoroacetic acid/methanol/water (4:1:8, v/v/v). The reaction mixture was stirred for 5 min at room temperature and then poured into ethyl acetate. The organic layer was washed with a 5% solution of sodium carbonate and brine, dried over $MgSO_4$, and concentrated. Product **4a** was purified by sublimation (T = 110 °C, P = 3 mmHg) and obtained in a yield of 97%. Mp 104−105 °C; $[\alpha]_D^{20}$ = −7.4° (methanol, *c* 1.0). IR (KBr, cm^{-1}): ν 3230 (OH), 2950, 2910, 2920 (C-H). ^{1}H-NMR ($CDCl_3$, ppm): δ 2.56 (s, 2H, OH), 3.33 (m, 4H, CH_2I), 3.93 (m, 2H, C*H*). MS(CI$^+$, *m/z*): 343 (M + 1), 215 (M − I).

(2*S*,3*S*)-1,4-Diiodobutane-2,3-diol, 4b. Compound **4b** was synthesized starting from **3b**[12] by using the same procedure as described for compound **4a**. A white solid was obtained in 96% yield. Mp 105 °C; $[\alpha]_D^{20}$ = +7.6° (methanol, *c* 1.0).

(2*R*,3*S*)-1,4-Diiodobutane-2,3-diol, 4c. A solution of **2c** (870 mg, 2.5 mmol) and NaI (1.49 g, 9.3 mmol) in butanone (200 mL) was heated under reflux for 48 h. The reaction mixture was filtered, and the filtrate was concentrated in vacuo. The residue was dissolved in ethyl acetate and washed with aqueous 10% NaS_2O_3 and brine. After drying over $MgSO_4$ and evaporation of the solvent, a diastereomeric mixture of **3c** was obtained to which trifluoroacetic acid/methanol/water (4:1:8, v/v/v) was added. The reaction mixture was stirred for 48 h at room temperature and then poured into ethyl acetate. The organic layer was washed with an aqueous 5% solution of Na_2CO_3 and brine, dried over $MgSO_4$, and concentrated. After crystallization from chloroform, **4c** was obtained in a yield of 94%. Mp 129−131 °C. Anal. ($C_4H_8O_2I_2$): C, H, Calcd: 14.05, 2.36. Found: 14.43, 2.43. IR (KBr, cm^{-1}): ν 3250 (OH), 2910, 2850 (C-H). ^{1}H-NMR ($CDCl_3$/CD_3OD, ppm): δ 3.25 (m, 2H, C*H*), 3.50 (m, 4H, CH_2). MS (EI$^+$, *m/z*): 342 (M^+), 215 (M − I).

(2*R*,3*R*)-1,4-Iodobutane-2,3-diyl Dioctadecanoate, 5a. Stearoyl chloride (3.5 g, 11.5 mmol) in dry ether was added at 0 °C to a solution of **4a** (0.85 g, 2.5 mmol) in dry diethyl ether (34 mL) and dry pyridine (4.3 mL). After standing for 24 h at room temperature, the reaction mixture was poured into ice water and extracted with diethyl ether. The organic layer was washed with aqueous 2 N H_2SO_4 and with a saturated solution of $Na_2S_2O_3$, dried over $MgSO_4$ and concentrated. The product **5a** crystallized from acetonitrile and was isolated as a white solid in 97% yield. Mp 54−56 °C.[25] $[\alpha]_D^{20}$= +5.3° (CH_2Cl_2, *c* 1.0). IR (KBr, cm^{-1}): ν 2950, 2910, 2850 (C-H), 1740 (C=O). ^{1}H-NMR ($CDCl_3$, ppm): δ 0.88 (t, 6H, CH_3, J = 6.7 Hz), 1.25 (m, 56H, $CH_2(CH_2)_{14}CH_3$), 1.56 (m, 4H, C(O)CH_2CH_2), 2.31 (t, 4H, C(O)CH_2, J = 7.5 Hz), 3.22 (d, 4H, CH_2I, J = 5.8 Hz), 4.66 (m, 2H, C*H*). ^{13}C-NMR {H}($CDCl_3$, ppm): δ 9.3 CH_2I, 13.9−34.11 (*C*-stearoyl), 72.0 (*C*H), 172.7 (*C*=O). MS (FB$^+$, *m/z*): 875 (M + 1), 747 (M − I).

(2*S*,3*S*)-1,4-Diiodobutane-2,3-diyl Dioctadecanoate, 5b. Compound **5b** was synthesized starting from **4b** using the same procedure as described for compound **5a**. A white solid was obtained in 96% yield. Mp 54−56 °C.[25] $[\alpha]_D^{20}$ = −6.8° (CH_2Cl_2, *c* 1.0).

(2*S*,3*R*)-1,4-Diiodobutane-2,3-diyl Dioctadecanoate, 5c. Compound **5c** was synthesized starting from **4c** using the same procedure as described for compound **5a**. A white solid was obtained in 90% yield. Mp 79−81 °C.[25] Anal. ($C_{40}H_{76}O_4I_2$): C, H, Calcd: 54.92, 8.76. Found: 55.47, 8.79. IR (KBr, cm^{-1}): ν 2950, 2910, 2840 (C−H), 1740 (C=O). ^{1}H-NMR ($CDCl_3$, ppm): δ 0.88 (t, 6H, CH_3, J = 6.7 Hz), 1.25 (m, 56H $CH_2(CH_2)_{14}CH_3$), 1.66 (m, 4H, C(O)CH_2CH_2), 2,37 (t, 4H, C(O)CH_2, J = 7.5 Hz), 3.30 (dd, AA′*XX*′YY′, 2H, CH_2I), 3.30 (dd, AA′XX′*YY*′, 2H, CH_2I), 4.86 (m, *AA*′XX′YY′, 2H, C*H*). MS (FB$^+$, *m/z*): 897 (M + Na$^+$), 747 (M − I).

(2*R*,3*R*)-Di(octadecanoyloxy)butane-1,4-diyl Bis(dibenzylphosphate), 6a. To a solution of **5a** (2.7 g, 3.0 mmol) in dry toluene (40 mL) was added silver dibenzyl phosphate[16] (6.6 mmol) while stirring under argon. The mixture was heated under reflux for 4 h with exclusion of light. The suspension was filtered over Hyflo, and the filtrate was concentrated under reduced pressure. After flash chromatography (silicagel, hexane/ethyl acetate = 7/3, v/v) the product **6a** was obtained as a colorless oil and crystallized from its acetonitrile solution (yield 85%). Mp 44−45 °C; $[\alpha]_D^{20}$ = −1.69° (CH_2Cl_2, *c* 1.0). IR (KBr, cm^{-1}): ν 3090, 3060, 3030 (C−H aryl), 2920, 2840 (C−H), 1745 (C=O), 1285 (P=O), 1010 (P−O−C). ^{1}H-NMR ($CDCl_3$, ppm): δ 0.88 (t, 6H, CH_3, J = 6.7 Hz), 1.25 (m, 56H $CH_2(CH_2)_{14}CH_3$), 1.56 (m, 4H, C(O)CH_2CH_2), 2.31 (t, 4H, C(O)CH_2 J = 7.5 Hz), 4.12 (m, 4H, CHCH_2O), 5.07 (dd, 8H, CH_2Bz, J_{P-H} = 8.4 Hz, J_{H-H} = 1.0 Hz) 5.28 (m, 2H, C*H*), 7.37 (s, 20H, C_6H_5). ^{31}P-NMR {H}($CDCl_3$, ppm): δ −3.06. ^{13}C-NMR {H}(acetone D^6, ppm): δ 14.9−35.1 (*C*-stearoyl), 66.6 (CH_2O, J_{P-C} = 5.5 Hz), 70.5 (CH_2Bz), 71.2 (*C*H), 128.2, 129.8, 129.9, 137.6, 138.1 (C_6H_5), 173.6 (*C*=O). MS (FB$^+$, *m/z*): 897 (M − HOP(O)(OBz)$_2$).

(2*S*,3*S*)-Di(octadecanoyloxy)butane-1,4-diyl Bis(dibenzylphosphate), 6b. Compound **6b** was synthesized starting from **5b** using the same procedure as described for compound **6a**. Mp 44−45 °C. Identical spectroscopic data were obtained as described for **6a**, except for the optical rotation: $[\alpha]_D^{20}$ = +1.58° (CH_2Cl_2, *c* 1.0).

(23) Dittmer, J. C. Lester, R. L. *J. Lipid Res.* **1964**, *5*, 126.
(24) Knight, R. H.; Young, L. *Biochem. J.* **1981**, *70*, 111.

(25) This melting point range suggests the presence of impurities. They could not be removed despite several attempts to obtain analytically pure material. It was then decided to purify the compound at a later stage in the synthetic sequence.

(2*S*,3*R*)-Di(octadecanoyloxy)butane-1,4-diyl Bis(dibenzylphosphate), 6c. Compound **6c** was synthesized in 51% yield, starting from **5c** by the same procedure as described for compound **5a**. Mp 53−54 °C. Anal. ($C_{68}H_{104}O_{12}P_2$) C, H, Calcd: 69.48 8.92. Found: 68.99, 8.77. IR (KBr, cm^{-1}): ν 3090, 3060, 3030 (C-H aryl), 2940, 2910, 2840 (C−H), 1725 (C=O), 1250 (P=O), 1020 (P−O−C). ^{1}H-NMR ($CDCl_3$, ppm): δ 0.88 (t, 6H, CH_3, J = 6.7 Hz), 1.25 (m, 56H $CH_2(CH_2)_{14}CH_3$), 1.53 (m, 4H, $C(O)CH_2CH_2$), 2,22 (t, 4H, $C(O)CH_2$, J = 7.5 Hz), 4.04 (m, 2H, $2CHCH_aH_bO$), 4.16 (m, 2H, $2CHCH_aH_bO$) 4.99 (m, 8H, CH_2Bz) 5.18 (br.s, 2H, CH), 7.37 (s, 20H, C_6H_5). MS (FB^+, m/z): 897 (M − $HOP(O)(OBz)_2$).

Sodium (2*R*,3*R*)-Di(octadecanoyloxy)butane-1,4-diyl Bisphosphate, 1a. The tetrabenzyl ester **6a** (500 mg, 0.6 mmol), dissolved in ethanol (40 mL), was subjected to hydrogenolysis for 0.5 h with Pd-(C) as the catalyst. The catalyst was filtered off using a small RP-2 column, and the filtrate was concentrated in vacuo. The residue was dissolved in distilled water with the aid of an aqueous 0.05 N solution of NaOH (36 mL), treated with Dowex 50WX20 (sodium form), and lyophilized. The product **1a** was purified by reversed phase chromatography (RP 2, methanol/water), lyophilized, and subsequently dried over P_2O_5 at 90 °C for 8 h. The yield was 61%. R_f = 0.48 (BuOH/AcOH/H_2O = 4/1/1). Mp > 200 °C dec. Anal.[26] ($C_{40}H_{76}P_2O_{12}Na_4 \cdot 2^1/_2H_2O$): C, H, Calcd 50.66, 8.62. Found: 50.68, 8.85. IR (KBr, cm^{-1}); ν 2950, 2910, 2860 (C−H), 1735 (C=O), 1200 (P=O). ^{31}P-NMR{H}(D_2O, ppm): δ −2.27.

Sodium (2*S*,3*S*)-Di(octadecanoyloxy)butane-1,4-diyl Bisphosphate, 1b. Compound **1b** was synthesized starting from **6b** using the same procedure as described for compound **1a** and obtained as an amorphous powder in 63% yield. Mp > 200 °C dec. Anal.[26] ($C_{40}H_{76}P_2O_{12}Na_4 \cdot 1^1/_2H_2O$): C, H, Calcd 51.64, 8.57. Found: 50.53 8.43. Spectroscopic data were identical to those given for **1a**.

Sodium (2*R*,3*S*)-Di(octadecanoyloxy)butane-1,4-diyl Bisphosphate, 1c. Compound **1c** was synthesized starting from **6c** using the same procedure as described for compound **1a**. The product was obtained as an amorphous powder in 97% yield (R_f = 0.40; BuOH/AcOH/H_2O = 4/1/1, v/v/v). Mp > 200 °C dec. Anal.[26] ($C_{40}H_{76}P_2O_{12}Na_4 \cdot 2H_2O$): C, H, Calcd 51.15, 8.59. Found: 50.63, 8.35. IR (KBr, cm^{-1}): ν 2950, 2910, 2860 (C−H), 1735 (C=O), 1200 (P=O). ^{31}P-NMR{H}(D_2O, ppm): δ −2.85.

Sample Preparation. Typically 1.0 μmol of a surfactant was suspended in 1.0 mL of 2 mM PIPES (piperazine-*N*,*N*′-bis[2-ethanesulfonic acid] buffer of pH = 7.0 by sonication at 70 °C in a bath type sonicator (Transsonic digital; level 9, degas) for 1 h. Calcium ion complexes were prepared by adding 1.0 mL of a PIPES buffer containing 1.0 mM $CaCl_2$ at 70 °C to a freshly prepared vesicle dispersion of the surfactant. These samples were kept at 70 °C for 2 h and then allowed to cool to room temperature. The samples were left overnight at room temperature before use, except when the fusion and fission of vesicles were monitored.

(26) Due to the hygroscopic character of these compounds varying amounts of water of crystallization had to be taken into account. The purity of these compounds was further checked by HPLC (Partisil SAX column, UV detection at 215 nm, eluent: 0.1 M KH_2PO_4/H_3PO_4 buffer of pH = 3).

Electron Microscopy. Freeze-fractured samples were prepared by bringing a drop of the dispersion onto a golden microscope grid (150 mesh), placed between two copper plates and fixated in supercooled liquid nitrogen. Sample holders were placed in a Balzers Freeze Etching System BAF 400 D at 10^{-7} Torr and heated to −105 °C. After fracturing, the samples were etched for 1 min (ΔT = 20°), shaded with Pt (layer thickness 2 nm), and covered with carbon (layer thickness 20 nm). Replicas were allowed to warm up to room temperature, left on 20% chromic acid for 16 h and rinsed with water. Negatively stained samples were prepared by bringing a drop of the dispersion onto a Formvar coated copper grid, kept at 4 °C. After 2 min the excess of dispersion was removed, and the sample was stained with a 2% (w/w) uranyl acetate solution.

After preparation the grids were allowed to dry and studied under a Philips TEM 201 microscope (60 kV).

DSC. Thermograms were recorded using a Perkin & Elmer DSC7 instrument. Samples were prepared as described above. Typically 50 μL was transferred into a stainless steel large volume pan (75 μL) and left overnight. After incubation for 15 min at 0 °C, heating runs were recorded from 0−100 °C.

Powder Diffraction. Samples were prepared in a desiccator, by placing a drop of the suspension on a silicon single crystal. Subsequent evacuation caused the freezing of the sample, and after sublimation of the ice the sample was placed in a Philips PW1710 diffractometer equipped with a Cu LFF X-ray tube operating at 40 kV and 55 mA. Experiments were carried out between 3 and 60°, using a step width of 0.005°.

Monolayer Experiments. Isotherms were recorded on a thermostated, home-built trough (140 × 210 mm). The surface pressure was measured using Wilhelmy plates mounted on a Trans-Tek transducer (Connecticut USA). On the subphase 150 μL of a chloroform solution (0.3−0.5 mg/mL) of the surfactant was spread and allowed to evaporate for 10 min. The rate of compression was 7.0 cm^2/min. The surface of compressed monolayers was studied with a Brewster Angle Microscope (NFT BAM-1) equipped with a 10 mW He-Ne laser with a beam diameter of 0.68 mm operating at 632.8 nm. Reflections were detected using a CCD camera, and images were recorded on a Panasonic superVHS video recorder.

Acknowledgment. The authors wish to thank H. P. M. Geurts (Department of Electron Microscopy, University of Nijmegen) for assistance in performing electron microscopy experiments and Professor A. E. Beezer (University of Kent) for helpful discussions.

Supporting Information Available: Electron micrographs of **1a** and powder diffraction patterns of agregates of **1b** and **1c**, before and after addition of calcium ions(3 pages). See any current masthead page for ordering and Internet access instructions.

JA962303S